China Ocean Eng., 2017, Vol. 31, No. 3, P. 341–349
DOI: 10.1007/s13344-017-0040-3, ISSN 0890-5487
http://www.chinaoceanengin.cn/ E-mail: coe@nhri.cn

Wave Interactions with Multiple Semi-Immersed Jarlan-Type Perforated Breakwaters

Moussa S. ELBISY*

Civil Engineering Department, College of Engineering and Islamic Architecture, Umm Al-Qura University, Makkah 22195, Saudi Arabia

Received January 28, 2016; revised May 30, 2016; accepted June 28, 2016

Abstract

This study examines wave interactions with multiple semi-immersed Jarlan-type perforated breakwaters. A numerical model based on linear wave theory and an eigenfunction expansion method has been developed to study the hydrodynamic characteristics of breakwaters. The numerical results show a good agreement with previous analytical results and experimental data for limiting cases of double partially immersed impermeable walls and double and triple Jarlan-type breakwaters. The wave transmission coefficient C_T; reflection coefficient C_R, and energy dissipation coefficient C_E coefficients and the horizontal wave force exerted on the front and rear walls are examined. The results show that C_R reaches the maximum value when $B/L = 0.46n$ while it is smallest when $B/L=0.46n+0.24$ (n=0, 1, 2,...). An economical triple semi-immersed Jarlan-type perforated breakwater can be designed with $B/L = 0.25$ and C_R and C_T ranging from 0.25 to 0.32 by choosing a relative draft d/h of 0.35 and a permeability parameter of the perforated front walls being 0.5 for an incident wave number kh nearly equal to 2.0. The triple semi-immersed Jarlan-type perforated breakwaters with significantly reduced C_R, will enhance the structure's wave absorption ability, and lead to smaller wave forces compared with the double one. The proposed model may be used to predict the response of a structure in the preliminary design stage for practical engineering.

Key words: Jarlan-type perforated breakwaters, analytical solution, eigenfunction, least squares technique

Citation: Elbisy, M. S., 2017. Wave interactions with multiple semi-immersed Jarlan-type perforated breakwaters. China Ocean Eng., 31(3): 341–349, doi: 10.1007/s13344-017-0040-3

1 Introduction

Breakwaters are mainly used to protect coasts from erosion, protect harbor facilities, and provide a calm basin for ships by reducing wave-induced disturbances. Rubble mound breakwaters are the oldest type of breakwaters. They have been widely used to shelter harbors. Caisson breakwaters are advantageous over rubble mound breakwaters as they require less space, material, and time for construction. However, caisson breakwaters reflect the incoming wave energy, and thus causing erosion at the breakwater toe.

Researchers have attempted to solve the problem of wave reflection and scouring at the breakwater toe by using perforated walls. Perforated breakwaters were first introduced by Jarlan (1961). He proposed a breakwater with a perforated front wall and a solid rear wall. Since then, several researchers have introduced several modifications to Jarlan-type perforated breakwaters to improve their hydraulic performance.

Kondo (1979) presented an analytical approach based on long wave theory to estimate C_R and C_T of double and triple Jarlan-type perforated breakwaters. Tanimoto and Yoshimoto (1982) theoretically and experimentally studied the reflection properties of partially perforated caissons. Twu and Lin (1991) examined the reflection of a finite number of porous plates. The authors concluded that the spacing between adjacent porous plates and the alignment of these plates significantly affects wave reflection. Fugazza and Natale (1992) analyzed the wave attenuation produced by the permeable structure and proposed design formulae for an optimized hydraulic design of Jarlan-type breakwaters.

Bennet et al. (1992) theoretically and experimentally studied C_R of a screen breakwater. Losada et al. (1993) used linear theory for water obliquely impinging on dissipative multilayered media to evaluate C_R and C_T. The results indicated that C_R decreases with the increasing number of absorber units. Suh and Park (1995) developed an analytical model to predict C_R of a fully perforated wall breakwater mounted on a rubble mound foundation; later, Suh et al. (2001, 2006) extended this model to random waves and a partially perforated wall caisson.

Cox et al. (1998) introduced a double semi-immersed Jarlan-type perforated breakwater. Their researches showed

*Corresponding author. E-mail: mselbisy@uqu.edu.sa

that with a suitable design, C_R and C_T of short waves can be smaller than 0.3.

Isaacson et al. (1998) theoretically studied C_R, wave run-up, and wave force for a breakwater consisting of a perforated front wall, an impermeable back wall, and a rock-filled core.

Brossard et al. (2003) proposed a semi-immersed caisson breakwater with a perforated front wall and demonstrated that both C_R and C_T of the breakwater could be small. Liu et al. (2007) studied C_R of obliquely incident waves for an infinite array of partially perforated Jarlan-type breakwaters. Garrido and Medina (2006) experimentally investigated slotted and perforated double and triple Jarlan-type breakwaters under regular and random waves and developed a nonlinear relationship between C_R and the structural and incident wave conditions.

Bergmann and Omeraci (2008) experimentally studied double-chambered breakwaters. They revealed that for effective wave damping, the relative wave chamber width (B/L) should exceed 0.3. Krishnakumar et al. (2009) experimentally investigated wave interactions with a double-chambered breakwater system consisting of two wave screens placed on the seaward side of an impermeable vertical wall. The authors concluded that at larger and smaller draft to wavelength ratios (d/L), the reflection is reduced by approximately 40% and 60%, respectively.

Molin et al. (2009) indicated that C_R of semi-immersed caissons can be greatly reduced by adding perforated walls. Liu and Li (2011) developed an analytical solution for describing the hydrodynamic performance of double semi-immersed Jarlan-type perforated breakwaters. They presented the optimal design parameters for the breakwater.

Using wave scattering based on eigenfunction expansions, Liu et al. (2015) studied wave interactions with a semi-immersed breakwater consisting of a perforated front wall, a solid rear wall, and a horizontal perforated plate between the two walls. In addition, they experimentally investigated C_R and C_T of the breakwater. The new breakwater was found to give a better wave-absorbing performance and smaller wave forces.

By extending Liu and Li's (2011) model, this study developed a mathematical model to investigate the hydrodynamic performance of multiple semi-immersed Jarlan-type perforated breakwaters. The studied breakwater consists of a seaward multi-perforated wall and a shoreward impermeable wall. All walls extend from above the seawater level to a distance above the seabed.

2 Mathematical formulation

Consider the multiple rows of the two-dimensional multiple semi-immersed Jarlan-type perforated breakwater sketched in Fig. 1, it consists of "J–1" seaward perforated walls and a shoreward impermeable wall "J" at a constant water depth h. The draft of the j-th breakwater is d_j, in

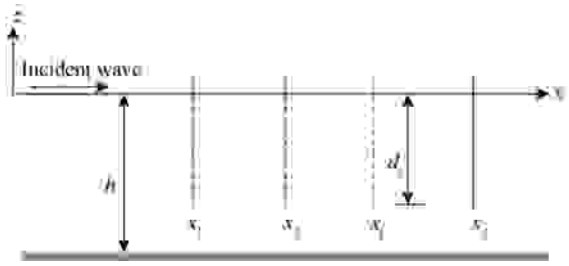

Fig. 1. Sketch-sectional view of the domains.

which b_j is the thickness of the j-th wall. A Cartesian coordinate system (x, z) is defined with the positive x-axis in the direction of wave propagation from a point in front of the first wall and the z-axis in the upward vertical direction. The center of the j-th wall is located at $x=x_j$.

The fluid is assumed incompressible and inviscid and the flow being irrotational. A velocity potential $\Phi(x, z, t)$ for the monochromatic wave propagating with the angular frequency ω over the water depth h can be expressed as:

$$\Phi_j(x,z,t) = \mathrm{Re}\left[\phi_j(x,z)\,\mathrm{e}^{-\mathrm{i}\omega t}\right], \tag{1}$$

where Re represents the real part of the complex expression in [ ], ϕ is the spatial velocity potential, $\mathrm{i}=\sqrt{-1}$, ω is the angular frequency, t is time, and g is the gravitational acceleration. In different regions, the spatial potentials satisfy the Laplace equation:

$$\frac{\partial^2\phi_j}{\partial x^2}+\frac{\partial^2\phi_j}{\partial z^2}=0 \quad \text{for} \quad j=0,1,2,...,J, \tag{2}$$

where the subscript j represents variables with respect to the region j. The potentials must satisfy the following boundary conditions:

$$\frac{\partial\phi_j}{\partial z}-\frac{\omega^2}{g}\phi_j=0, \quad \text{at } z=0, \quad j=0,1,2,...,J; \tag{3}$$

$$\frac{\partial\phi_j}{\partial z}=0, \quad \text{at } z=-h, \quad j=0,1,2,...,J; \tag{4}$$

$$\lim_{x\to-\infty}\left(\frac{\partial\phi_0}{\partial z}+\mathrm{i}k_0\phi_0\right)=0; \tag{5}$$

$$\lim_{x\to+\infty}\left(\frac{\partial\phi_J}{\partial z}-\mathrm{i}k_0\phi_J\right)=0. \tag{6}$$

In addition, the boundary conditions at the breakwater walls are

$$\frac{\partial\phi_{j-1}}{\partial x}=\frac{\partial\phi_j}{\partial x}=\mathrm{i}k_0G_j\left(\phi_{j-1}-\phi_j\right), x=x_j, \quad -d_j\leqslant z\leqslant 0, \quad j=1,2,...,J-1; \tag{7}$$

$$\frac{\partial\phi_{j-1}}{\partial x}=\frac{\partial\phi_j}{\partial x}, x=x_j, \quad -h\leqslant z\leqslant -d_j, \quad j=1,2,...,J-1; \tag{8}$$

$$\phi_{j-1}=\phi_j, x=x_j, \ -h\leqslant z\leqslant -d_j, \ j=1,2,...,J-1; \tag{9}$$

$$\frac{\partial\phi_{J-1}}{\partial x}=\frac{\partial\phi_J}{\partial x}=0, x=x_J, \quad -d_J\leqslant z\leqslant 0; \tag{10}$$

$$\frac{\partial\phi_{J-1}}{\partial x}=\frac{\partial\phi_J}{\partial x},\ x=x_J,\quad -h\leqslant z\leqslant -d_J; \tag{11}$$

$$\phi_{J-1}=\phi_J,\ x=x_J,\quad -h\leqslant z\leqslant -d_J, \tag{12}$$

where G_j is the permeability parameter of the j-th permeable wall (Chwang and Li, 1983; Yu, 1995).

In this study, the formula proposed by Yu (1995) is followed. G_j is given by

$$G_j=\frac{\varepsilon_j}{b_j(f_j-\mathrm{i}s_j)}=\left|G_j\right|\mathrm{e}^{\mathrm{i}\theta_j},\quad 0\leqslant\theta_j\leqslant\pi/2 \tag{13}$$

where θ_j is the argument of the complex G_j, ε_j is the geometrical porosity of the j-th wall, b_j is its thickness, f_j is the friction coefficient, and s_j is the inertial coefficient given by

$$s_j=1+C_{\mathrm{m}}\left(\frac{1-\varepsilon_j}{\varepsilon_j}\right), \tag{14}$$

where C_{m} is the added mass coefficient, and f_j is the linearized resistance coefficient through the permeable wall. f_j in Eq. (13) can be calculated by the following formula (Li et al., 2006):

$$f_j=-3338.7\left(b_j/h\right)^2+82.769\left(b_j/h\right)+8.711,$$
$$0.0094\leqslant\left(b_j/h\right)+8.711\leqslant 0.05.$$

3 Analytical solutions

Expressions for $\phi_j(j=0,1,2,...,J)$ that satisfy the seabed, free surface, and boundary conditions, as well as the abovementioned boundary conditions along $x=x_i$, may be developed in terms of coefficients A_{jm} and B_{jm}, which are the component waves propagating forward and backward, respectively. The first subscript (j) indicates the row of the wall, whereas the second one (m) indicates the wave component. The reduced velocity potentials ϕ_j are obtained using the eigenfunction expansion method, as in Isaacson et al. (1998) and Suh et al. (2006). The velocity potentials are expressed as a series of an infinite number of solutions. The solutions to Eq. (2) satisfying the boundary conditions, Eq. (3) to Eq. (6), are given by

$$\phi_0=-\frac{\mathrm{i}gH_i}{2\omega}\left[Z_0(z)\mathrm{e}^{-\mu_0(x-x_1)}+\sum_{m=0}^{\infty}B_{0m}Z_m(z)\mathrm{e}^{\mu_m(x-x_1)}\right]$$
$$\text{at } x\leqslant x_1; \tag{15}$$

$$\phi_j=-\frac{\mathrm{i}gH_i}{2\omega}\left[\sum_{m=0}^{\infty}A_{jm}Z_m(z)\mathrm{e}^{-\mu_m(x-x_j)}\right.$$
$$\left.+\sum_{m=0}^{\infty}B_{jm}Z_m(z)\mathrm{e}^{\mu_m(x-x_{j+1})}\right]\text{at } x_j\leqslant x\leqslant x_{j+1},$$
$$j=1,2,...,J-1; \tag{16}$$

$$\phi_J=-\frac{\mathrm{i}gH_i}{2\omega}\left[\sum_{m=0}^{\infty}A_{Jm}Z_m(z)\mathrm{e}^{-\mu_m(x-x_J)}\right]\text{at } x\geqslant x_J, \tag{17}$$

where the pair of imaginary roots $\mu_0=\pm\mathrm{i}k$ for propagating waves are the solution to the dispersion relation, i.e. $\omega^2=g\mu_0\tanh(\mu_0h)$. Let $\mu_0=-\mathrm{i}k$ such that the propagating waves in Eqs. (15)–(17) correspond to the reflected and transmitted waves. The wave numbers μ_m are the solution to the dispersion relation, i.e., $\omega^2=-g\mu_m\tan(\mu_mh)$, which has an infinite discrete set of real roots $\pm\mu_m$ ($m\geqslant 1$) for nonpropagating evanescent waves. In addition, let the positive roots for $m\geqslant 1$ be such that the nonpropagating waves die out exponentially with the increasing distance from the wall.

In Eqs. (15)–(17), the depth-dependent functions $Z_0(z), Z_0'(z), Z_m(z)$, and $Z_m'(z)$ are given by

$$Z_0(z)=-\frac{gH_i}{2\omega}\frac{\mathrm{e}^{-\mathrm{i}\omega t}}{\cosh(k_0h)}\cosh\left[\mu_0(h+z)\right] \tag{18}$$

and

$$Z_m(z)=-\frac{gH_i}{2\omega}\frac{\mathrm{e}^{-\mathrm{i}\omega t}}{\cos(k_mh)}\cos[\mu_m(h+z)],\quad m=1,2,... \tag{19}$$

To solve the unknown coefficients of Eqs. (15)–(17), they must automatically satisfy all relevant boundary conditions, i.e. Eqs. (7)–(12); for convenience, these matching boundary conditions are rewritten as:

$$\frac{\partial\phi_{j-1}}{\partial x}=\frac{\partial\phi_j}{\partial x},x=x_j,\quad -h\leqslant z\leqslant 0,\quad j=1,2,...,J-1; \tag{20}$$

$$\frac{\partial\phi_j}{\partial x}=\mathrm{i}k_0G_j\left(\phi_{j-1}-\phi_j\right),x=x_j,-d_j\leqslant z\leqslant 0,\ j=1,2,...,J-1; \tag{21}$$

$$\phi_{j-1}=\phi_j,x=x_j,\quad -h\leqslant z\leqslant -d_j,\quad j=1,2,...,J-1; \tag{22}$$

$$\frac{\partial\phi_{J-1}}{\partial x}=\frac{\partial\phi_J}{\partial x},x=x_J,\quad -h\leqslant z\leqslant 0; \tag{23}$$

$$\frac{\partial\phi_J}{\partial x}=0,x=x_J,\quad -d_J\leqslant z\leqslant 0; \tag{24}$$

$$\phi_{J-1}=\phi_J,x=x_J,\quad -h\leqslant z\leqslant -d_J. \tag{25}$$

The least squares technique, suggested by Dalrymple and Martin (1990), can be used to determine the coefficients B_{0m}, which requires the value of

$$\int_{-h}^{0}|P_1(z)|^2\,\mathrm{d}z=0 \tag{26}$$

to be minimized. Minimizing these integrals with respect to coefficient B_{0m} leads to

$$\int_{-h}^{0}P_1^*(z)\frac{\partial P_1(z)}{\partial B_{0m}}\,\mathrm{d}z=0,\qquad m=0,1,2,..., \tag{27}$$

where $P_1^*(z)$ is the complex conjugate of $P_1(z)$, and

$$\frac{\partial P_1^{-h\leqslant z\leqslant 0}(z)}{\partial B_{0m}}=\mu_mZ_m; \tag{28}$$

$$\frac{\partial P_1^{-d_1\leqslant z\leqslant 0}(z)}{\partial B_{0m}}=\mathrm{i}k_0G_1Z_m; \tag{29}$$

$$\frac{\partial P_1^{-h\leqslant z\leqslant -d_1}(z)}{\partial B_{0m}}=\mathrm{i}k_0G_1Z_m. \tag{30}$$

For $x=x_j$ ($j=1,2,...,J-1$)

$$\int_{-h}^{0} P_j^*(z)\frac{\partial P_j(z)}{\partial A_{(j-1)m}}\mathrm{d}z$$
$$= \int_{-h}^{0}\left[A^*_{(j-1)n}\mu_n^*\mu_m Z_n^* Z_m\left(\mathrm{e}^{-\mu_n\Delta x_{j-1}}\right)^*\mathrm{e}^{-\mu_m\Delta x_{j-1}}\right.$$
$$-B^*_{(j-1)n}\mu_n^*\mu_m Z_n^* Z_m\mathrm{e}^{-\mu_m\Delta x_{j-1}}$$
$$-A^*_{jn}\mu_n^*\mu_m Z_n^* Z_m\mathrm{e}^{-\mu_m\Delta x_{j-1}}$$
$$\left.+B^*_{jn}\mu_n^*\mu_m Z_n^* Z_m\left(\mathrm{e}^{-\mu_n\Delta x_j}\right)^*\mathrm{e}^{-\mu_m\Delta x_{j-1}}\right]\mathrm{d}z = 0. \quad (31)$$

Finally, for $x=x_J$,

$$\int_{-h}^{0} P_J^*(z)\frac{\partial P_J(z)}{\partial A_{(J-1)m}}\mathrm{d}z$$
$$= \left[-A^*_{(J-1)n}\mu_n^*\mu_m Z_n^* Z_m\left(\mathrm{e}^{-\mu_n\Delta x_{J-1}}\right)^*\mathrm{e}^{-\mu_m\Delta x_{J-1}}\right.$$
$$+B^*_{(J-1)n}\mu_n^*\mu_m Z_n^* Z_m\,\mathrm{e}^{-\mu_m\Delta x_{J-1}}$$
$$\left.+A^*_{Jn}\mu_n^*\mu_m Z_n^* Z_m\mathrm{e}^{-\mu_m\Delta x_{J-1}}\right]\mathrm{d}z = 0. \quad (32)$$

Once the wave potentials are calculated, the various engineering wave properties can be obtained. The reflection and transmission coefficients are given by

$$C_\mathrm{R} = |B_{00}|, \quad (33)$$

and

$$C_\mathrm{T} = |A_{J0}|. \quad (34)$$

The wave energy dissipation coefficient C_E is expressed as:

$$C_\mathrm{E} = 1 - C_\mathrm{R}^2 - C_\mathrm{T}^2. \quad (35)$$

The wave force on each wall can be calculated by integrating the wave pressure acting on both the upwave and downwave sides of the wall. The magnitude of the horizontal wave force on the unit width of the front wall, F_f, is expressed as:

$$F_\mathrm{f} = \mathrm{i}\rho\omega\int_{-\mathrm{d}}^{0}(\Phi_0 - \Phi_1)|_{x=x_1},$$
$$\mathrm{d}z = \frac{\rho g H}{2\mu_0 G}\left\{\sum_{m=0}^{\infty}(A_{1m})\frac{\sin(\mu_m h) - \sin[\mu_m(h-d)]}{\cos(\mu_m h)}\right\}. \quad (36)$$

The magnitude of the horizontal wave force on the unit width of the rear wall, F_r, is expressed as:

$$F_\mathrm{r} = \mathrm{i}\rho\omega\int_{-d}^{0}(\Phi_{J-1} - \Phi_J)|_{x=x_J},$$
$$\mathrm{d}z = \rho g H\left\{\sum_{m=1}^{\infty}\left(A_{Jm}\mathrm{e}^{-\mu_m(x_J - x_{J-1})} + B_{(J-1)m}\right)\right.$$
$$\left.\frac{\sin(\mu_m h) - \sin[\mu_m(h-d)]}{\mu_m\cos(\mu_m h)}\right\}. \quad (37)$$

The dimensionless wave forces C_{F_f} and C_{F_r} are expressed as:

$$C_{F_\mathrm{f}} = \frac{|F_\mathrm{f}|}{\rho g H h}; \quad (38)$$

$$C_{F_\mathrm{r}} = \frac{|F_\mathrm{r}|}{\rho g H h}. \quad (39)$$

4 Validation of the mathematical model

The effectiveness of the present model is validated by comparing the calculated results with previous analytical results by Horiguchi (1976), Natale (1983), Fugazza and Natale (1992), and Das et al. (1997) as well as previous experimental data of Kondo (1979) and Cox et al. (1998).

4.1 Comparisons with other theoretical models

For double partially immersed solid walls ($|G|$ for the perforated front wall is zero), the present calculated reflection coefficient was compared with the corresponding result of Das et al. (1997), as shown in Fig. 2. The calculated conditions are d/h=0.6 and B=2.0h. As shown in Fig. 2, the results obtained by the present model agree well with the analytical results of Das et al. (1997).

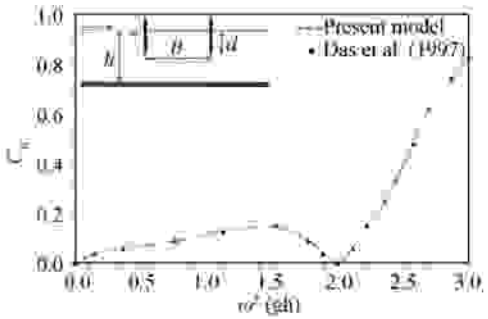

Fig. 2. Comparison between, the results of the present model and those of Das et al. (1997).

For a double Jarlan-type perforated breakwater, data from the theoretical results of Horiguchi (1976) and Natale (1983) are considered, in which the water depth h was 3.0 m, the wave height H was 1.0 m, the chamber width B was 4.0 m, d/h was 1.0, and the porosity of the perforated wall was ε=0.3. As shown in Fig. 3, the results of the present model are close to the theoretical results of Horiguchi (1976) and Natale (1983).

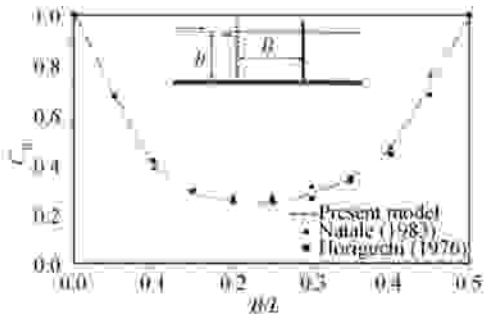

Fig. 3. Comparison between the results of the present model and those of Horiguchi (1976) and Natale (1983) for a double Jarlan-type perforated breakwater.

In addition, for a double Jarlan-type perforated breakwater, data from the theoretical results of Fugazza and Natale

(1992) are considered, in which the wave height H was 4.0 cm, the chamber width B was 0.5 m, d/h was 1.0, and the porosity of the perforated wall ε was 0.2. Fig. 4 shows that the present results agree reasonably well with the theoretical results of Fugazza and Natale (1992).

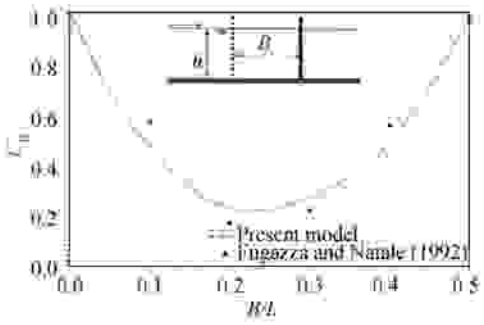

Fig. 4. Comparison between the results of the present model and those of Fugazza and Natale (1992) for a double Jarlan-type perforated breakwater.

4.2 Comparisons with experimental Data

The results of the present model for C_R of double semi-immersed Jarlan-type perforated breakwaters were validated by comparison with the results of Cox et al. (1998). In tests by Cox et al., ε was 20%, s was 1, b/h was 0.02, and d/h were 0.3 and 0.5. As shown in Fig. 5, the results obtained by the present model agree well with the experimental results of Cox et al. (1998).

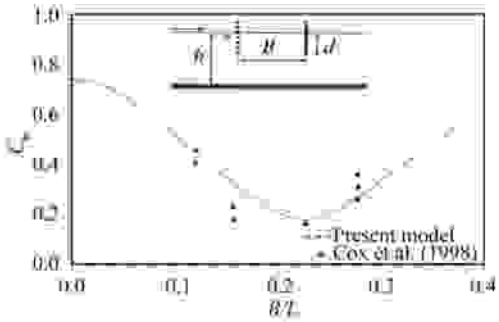

Fig. 5. Comparison between the results of the present model and those of Cox et al. (1998) for double semi-immersed Jarlan-type perforated breakwaters.

Next, the present model results for C_R of double and triple Jarlan-type perforated breakwaters were validated by comparison with the experimental results of Kondo (1997). The porosity of the perforated wall, ε, was 0.2. As shown in Figs. 6 and 7, the present results agree well with the experimental results of Kondo (1979).

5 Numerical examples

The relationships among C_R, C_T, and C_E of double semi-immersed Jarlan-type perforated breakwaters and the relative wave chamber width B/L for different values of the relative draft d/h (d/h=0.35, 0.5, 0.75, and 1.0) with kh=1.6,

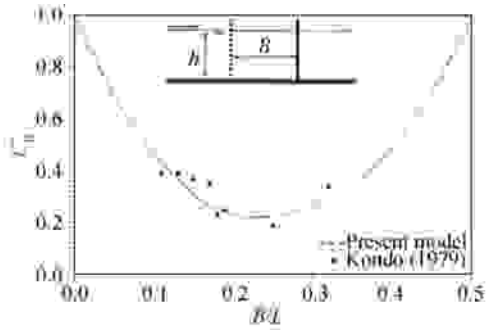

Fig. 6. Comparison between the results of the present model and those of Kondo (1979) for a double Jarlan-type perforated breakwater.

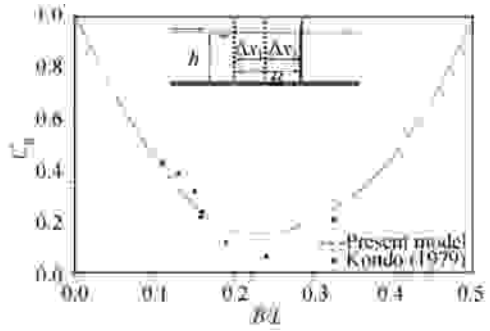

Fig. 7. Comparison between the results of the present model and those of Kondo (1979) for a triple Jarlan-type perforated breakwater.

G=0.5, and H/h=0.1 are shown in Fig. 8. Both C_R and C_T oscillate with changing B/L with the same trend. The mentioned effect is due to the dissipation of the wave's energy by the perforated front wall and the C_E oscillation with changing B/L. The maximum value of C_R appears when $B/L = 0.46n$ and its minimum value occurs when $B/L = 0.46n+0.24$ (n=0, 1, 2, ...). The maxima and minima of C_R curve are shifted to the left compared with that of the original bottom-standing Jarlan-type perforated breakwaters presented in Chwang and Dong (1984). Fig. 8 also represents the change in C_E against B/L with opposite maximum and minimum values compared with C_R and C_T. Furthermore, C_T decreases gradually with the increasing d/h.

Fig. 9 shows C_R, C_T, and C_E of double semi-immersed Jarlan-type perforated breakwaters against d/h for varied values of B/L (B/L=0, 0.25, 0.75, and 1.0) with kh=1.6, G=0.5, and H/h=0.1. From Fig. 9, it is obvious that C_T decreases with the increasing d/h. However, the variation in C_R with increasing d/h is related to B/L. That is, an increasing d/h does not necessarily lead to a larger C_R. It agrees with the results of Brossard et al. (2003) and Liu and Li (2011). It is also obvious that C_E increases with the increasing d/h until reaching a peak; after that, it becomes fixed, except in the case of B/L=0.5, where it decreases. Comparing the different curves in Fig. 9 shows that the values of B/L=0.25, d/h=0.35, B/L=0.75 and d/h=0.35 should be suitable for simultaneously obtaining smaller C_R and C_T values.

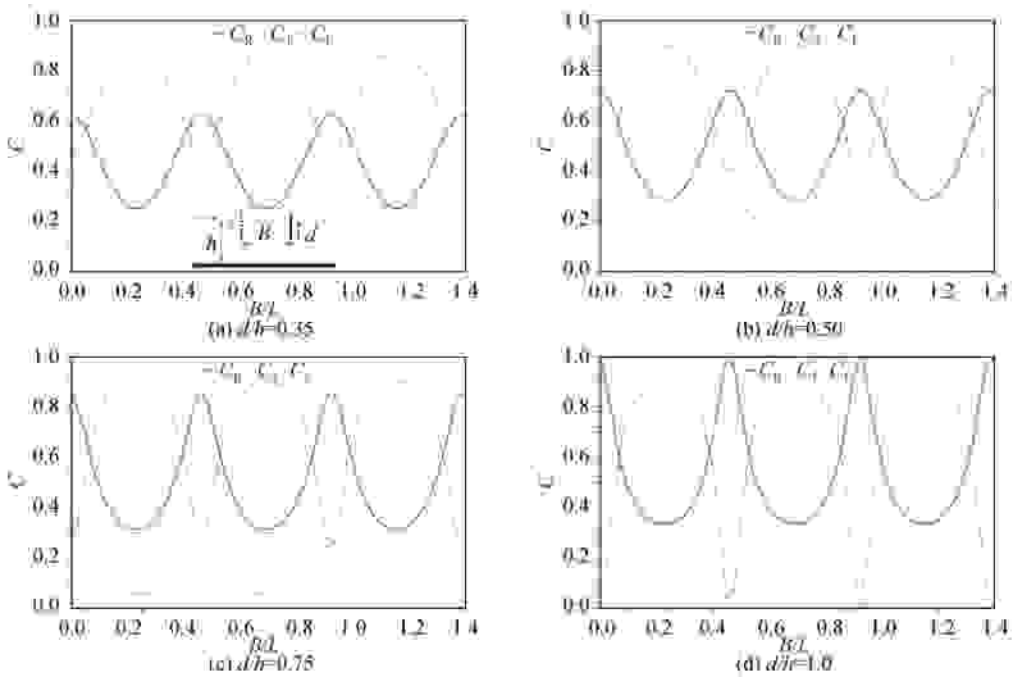

Fig. 8. Variation in C_R, C_T, and C_E of double semi-immersed Jarlan-type perforated breakwaters against B/L for different values of d/h with kh=1.6, G=0.5, and H/h=0.1.

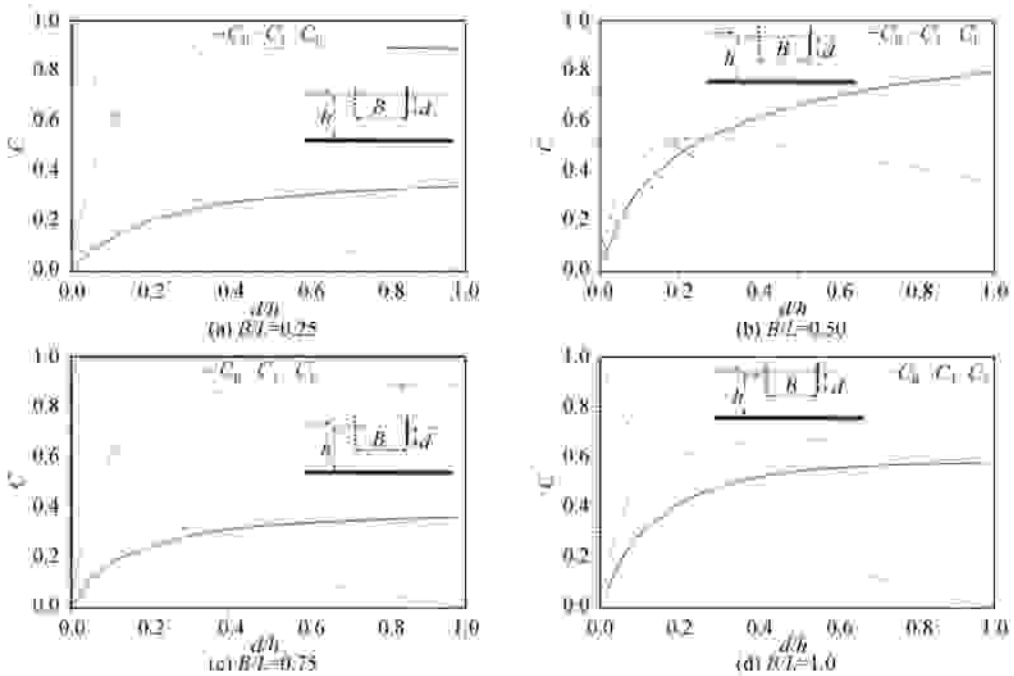

Fig. 9. Variation in C_R, C_T, and C_E of double semi-immersed Jarlan-type perforated breakwaters against d/h for different values of B/L with kh=1.6, G=0.5, and H/h=0.1.

The relationships among C_R, C_T, and C_E and B/L for different values of G (G=0.5, 1.0, and 2.0) at kh=1.6, H/h=0.1, and d/h=0.5 for double semi-immersed Jarlan-type perforated breakwaters are shown in Fig. 10. It can be observed that the variations in C_R and C_T with B/L are somewhat similar. The variation in C_E with B/L is just the opposite of that in C_R and C_T with B/L. Furthermore, it can be observed that the positions of the maximum and minimum values of C_R against B/L are not affected by G, which is similar to the results of Liu and Li (2011).

The variations in the horizontal wave force exerted on the front wall (C_{F_f}) and rear wall (C_{F_r}) against B/L for different values of G (0.5 and 2.0) with kh=1.6, d/h=0.5, and H/h=0.1 for double semi-immersed Jarlan-type perforated

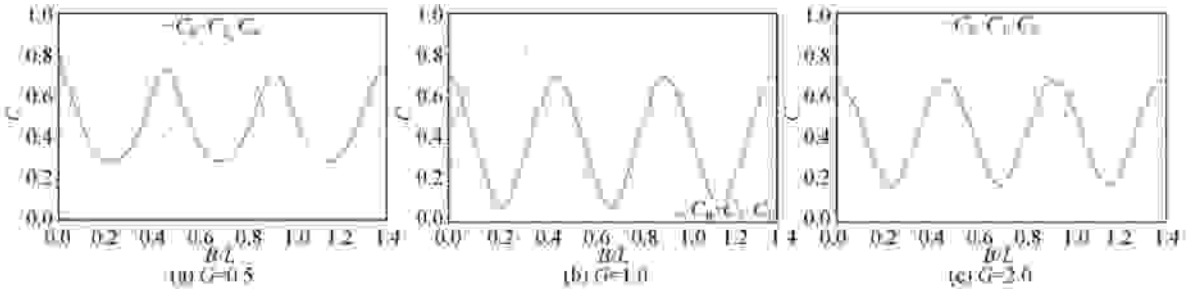

Fig. 10. Variation in C_R, C_T, and C_E of double semi-immersed Jarlan-type perforated breakwaters against B/L for different values of G with kh=1.6, d/h=0.5, and H/h=0.1.

breakwaters are shown in Fig. 11. It can be seen that C_{F_f} decreases as G increases. This might be because the increase in G allows more wave energy to pass through the porous front wall, and thus, less force is exerted on the front wall. The comparison between Fig. 10 and Fig. 11 shows that the maximum C_R corresponds with the minimum C_{F_f} and vice versa. This agrees with the results of Yip and Chwang (2000) and Liu and Li (2011). C_R and C_{F_f} can be related to the difference in the water level between the two sides of the perforated wall as follows: when C_R is maximum, the difference in the water level is very small, and hence, C_{F_f} is minimum. The opposite is also applicable: when C_R is minimum, the difference in the water level is very large, and hence, C_{F_f} is maximum. Moreover, the relationship between G and C_{F_r} can be observed from Fig. 11:

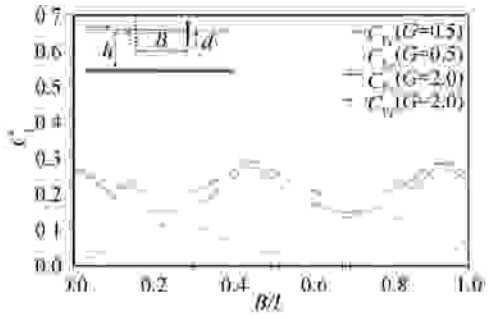

Fig. 11. Variation in C_{F_f} and C_{F_r} of double semi-immersed Jarlan-type perforated breakwaters against B/L for different values of G with kh=1.6, d/h=0.5, and H/h= 0.1.

as G increases, C_{F_r} increases. The variations in both C_{F_r} and C_T with B/L are similar. This can be observed in Figs. 10 and 11. This result agrees with the results of Liu and Li (2011).

The location of the middle wall between the front and rear walls is varied three times such that for the three trials, Δx_1=0.5h and Δx_2=1.5h, Δx_1=1.0h and Δx_2=1.0h, and Δx_1=1.5h and Δx_2=0.5h. Fig. 12 shows that the curves of C_R, C_T, and C_E against B/L are periodic, which is similar to that of a double semi-immersed Jarlan-type perforated breakwater. It is also clear that C_T and C_R follow the same trend while C_E shows an opposite trend. From the results, it can be concluded that the location of the middle wall has little effect on C_R, C_T, and C_E.

Comparing Figs. 12 and 8b reveals that the semi-immersed Jarlan-type perforated breakwaters show a significant reduction in the reflection coefficient values compared with the double semi-immersed Jarlan-type perforated breakwaters. This agrees with the results of Sawaragi and Iwata (1978), Kondo (1979), Fugazza and Natale (1992), Williams et al. (2000), Bergmann and Oumeraci (2000), Chen et al. (2002), Li et al. (2003), and Huang (2006).

The relationships among the C_R, C_T, and C_E of triple semi-immersed Jarlan-type perforated breakwaters and kh for different values of B/L (B/L=0.25, 0.5, and 0.75) with kh=1.6, H/h=0.1, $d//h$=0.25, and Δx_1=Δx_2=1.0h are shown in Fig. 13. It indicates that C_R increases with the increasing kh at a fixed B/L. Furthermore, C_T decreases with the increasing kh; that is, with increasing kh, the sheltering ability of

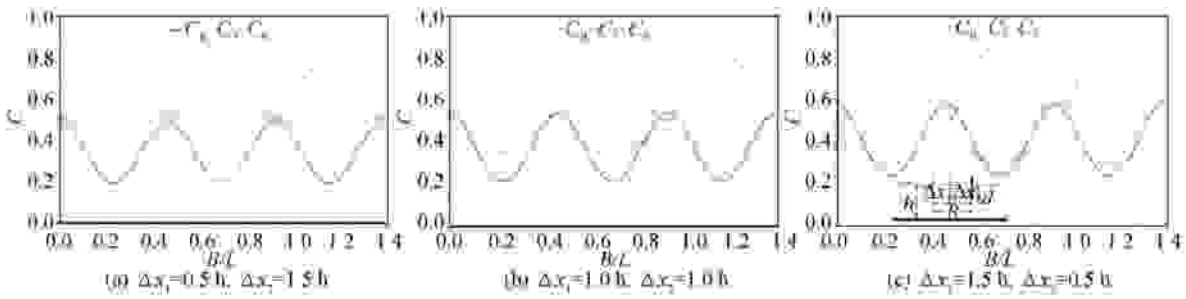

Fig. 12. Variation in C_R, C_T, and C_E of triple semi-immersed Jarlan-type perforated breakwaters against B/L for different values of the relative distance between the walls with kh=1.6, $d//h$=0.5, G=0.5, and H/h=0.1.

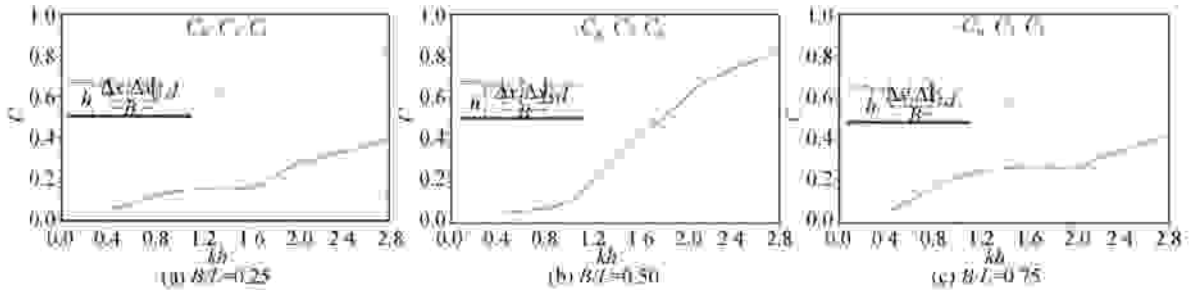

Fig. 13. Variation in C_R, C_T, and C_E of triple semi-immersed Jarlan-type perforated breakwaters against kh for different values of B/L with H/h=0.1, $d//h$=0.25, and $\Delta x_1=\Delta x_2$= 1.0h.

the breakwater increases. This agrees with the results of Liu and Li (2011) and Neelamani and Vedagiri (2002). Fig. 13 also shows that C_E increases with the increasing kh until reaching the peak point; after that, it decreases and the values of C_R and C_T range from 0.25 to 0.32 for kh=2:2.2 and B/L=0.25 and 0.75.

Fig. 14 presents the relationships among C_{F_f} and C_{F_r} and B/L for a triple semi-immersed Jarlan-type perforated breakwater with the following parameters: G=0.5 and 2.0, kh=1.6, d/h=0.5, $\Delta x_1=\Delta x_2$= 1.0h, and H/h= 0.1. Comparison between Fig. 14 and Fig. 12b shows that the variations in both C_{F_f} and C_R against B/L are opposite. The triple semi-immersed Jarlan-type perforated breakwaters were found to be very helpful in enhancing the structure's wave-absorbing ability compared with the double one. Moreover, Figs. 12b and 14 show that the variations in both C_{F_r} and C_T against B/L are similar.

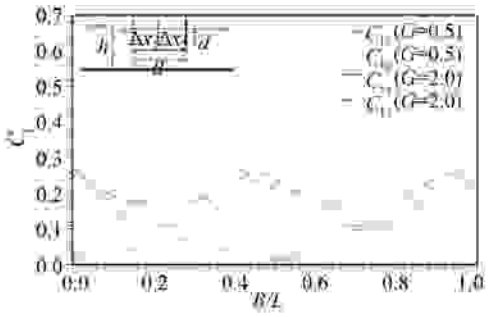

Fig. 14. Variations in C_{F_f} and C_{F_r} of triple semi-immersed Jarlan-type perforated breakwaters against B/L for different values of G with kh=1.6, d/h=0.5, $\Delta x_1=\Delta x_2$=1.0h, and H/h=0.1.

6 Conclusions

A mathematical model based on an eigenfunction expansion method and a least squares technique for linear waves has been developed to study the hydrodynamic performance of multiple semi-immersed Jarlan-type perforated breakwaters. The model is validated by comparing the predicted results with the analytical results of Horiguchi (1976), Natal (1983), Fugazza and Natale (1992), and Das et al. (1997) and the experimental data of Kondo (1979) and Cox et al. (1998). The comparisons showed that the results of the presented mathematical model agree reasonably well with the previous analytical results and experimental data. Thus, the model can be used to analyze the performance of multiple semi-immersed Jarlan-type perforated breakwaters.

Numerical examples show that C_R is maximum when B/L=0.46n while it is minimum when B/L=0.46n+0.24 (n=0, 1, 2, ...). It is also found that G does not affect the positions of the maximum or minimum values of C_R against B/L. However, as G increases, C_{F_f} decreases and C_{F_r} increases. The minimum value of C_R corresponds with the situation of the maximum horizontal force on the front wall and vice versa. The values of B/L=0.25 and d/h=0.35 and B/L=0.75 and d/h=0.35 should be suitable to obtain smaller C_R and C_T values.

In general, it is possible to construct a perforated breakwater with a smaller wave-absorbing chamber width and low C_R value by choosing suitable d/h and G. A small value of C_R can be obtained in a narrow range of B/L and with a small d/h. In addition, the sheltering ability of the breakwater increases with the increasing kh.

For triple breakwaters, the location of the middle wall between the front and rear walls has little effect on C_R, C_T, and C_E. The triple semi-immersed Jarlan-type perforated breakwaters significantly reduced C_R values compared with the double one. Moreover, the triple type was found to be very helpful in enhancing the structure's wave-absorbing ability compared with the double one.

In future work, more investigations should be carried out on multiple semi-immersed Jarlan-type perforated breakwaters with obliquely incident waves in cases of both absence and presence of sea currents.

References

Bennet, G.S., McIver, P. and Smallman, J.V., 1992. A mathematical model of a slotted wave screen breakwater, *Coast. Eng.*, 18(3), 231–249.

Bergmann, H. and Oumeraci, H., 2000. Wave loads on perforated Caisson breakwaters, *Proceedings of the 27th International Conference on Coastal Engineering*, Sydney, Australia, 1622–1635.

Bergmann, H. and Oumeraci, H., 2008. Wave induced water level elevation and pressure distribution at vertical perforated walls, *Proc.*

COPEDEC VII, *COPEDEC*, Dubai, United Arab Emirates.

Brossard, J., Jarno-Druaux, A., Marin, F. and Tabet-Aoul, E.H., 2003. Fixed absorbing semi immersed breakwater, *Coast. Eng.*, 49(1), 25–41.

Chen, X.F., Li, Y.C. and Sun, D.P., 2002. Regular waves acting on double-layered perforated caissons, *Proceedings of the 12th International Offshore and Polar Engineering Conference*, Kitakyushu, Japan, 736–743.

Chwang, A.T. and Li, W., 1983. A piston-type porous wavemaker theory, *J. Eng. Math.*, 17(4), 301–313.

Chwang, A.T. and Dong, Z.N., 1984. Wave trapping due to a porous plate, *Proceedings of the 15th ONR Symposium on Naval Hydrodynamics*, 407–414.

Cox, R.J., Horton, P.R. and Bettington, S.H., 1998. Double walled, low reflection wave barriers, *Proceedings of the 26th International Conference on Coastal Engineering*, Copenhagen, Denmark, 2221–2234.

Dalrymple, R.A. and Martin, P.A., 1990. Wave diffraction through offshore breakwaters, *J. Waterw. Port Coast Ocean Eng.*, 116(6), 727–741.

Das, P., Dolai, D.P. and Mandal, B.N., 1997. Oblique wave diffraction by parallel thin vertical barriers with gaps, *J. Waterw. Port Coast Ocean Eng.*, 123(4), 163–171.

Fugazza, M. and Natale, L., 1992. Hydraulic design of perforated breakwaters, *J. Waterw. Port Coast Ocean Eng.*, 118(1), 1–14.

Garrido, J.M. and Medina, J.R., 2006. Study of reflection of perforated vertical breakwaters, *Proceedings of the 30th International Conference on Coastal Engineering*, San Diego, California, USA, 4325–4336.

Horiguchi, T., 1976. *Wave Dissipation and Forces on A Perforated Caisson Breakwater*, Memoirs of Faculty of Tech., 26, Tokyo Metropolitan Univ., Tokyo, Japan.

Huang, Z.H., 2006. A method to study interactions between narrow-banded random waves and multi-chamber perforated structures, *Acta Mech. Sinica.*, 22(4), 285–292.

Isaacson, M., Baldwin, J., Allyn, N. and Cowdell, S., 1998. Design of a perforated breakwater, *Proc. Ports '98 Conf.*, California, USA, 1189–1198.

Jarlan, G.E., 1961. A perforated vertical breakwater, *Dock Harbour Auth.*, 41(486), 394–398.

Kondo, H., 1979. Analysis of breakwater having two porous walls, *Proc. Coastal Structures '79*, Reston, Virginia, USA, 962–977.

Krishnakumar, C., Sundar, V. and Sannasiraj, S.A., 2009. Attenuation of wave energy by double chambered breakwaters, *Advances in Water Resources and Hydraulic Engineering*, 1311–1315.

Li, Y.C., Dong, G.H., Liu, H.J. and Sun, D.P., 2003. The reflection of oblique incident waves by breakwaters with double-layered perforated wall, *Coast. Eng.*, 50(1), 47–60.

Li, Y.C., Liu, Y. and Teng, B., 2006. Porous effect parameter of thin permeable plates, *Coast. Eng. J.*, 48(4), 309–336.

Liu, Y., Li, Y.C. and Teng, B., 2007. The reflection of oblique waves by an infinite number of partially perforated caissons, *Ocean Eng.*, 34(14), 1965–1976.

Liu, Y. and Li, Y.C., 2011. Wave interaction with a wave absorbing double curtain-wall breakwater, *Ocean Eng.*, 38(10), 1237–1245.

Liu, Y., Yao, Z.L. and Li, H.J., 2015. Analytical and experimental studies on hydrodynamic performance of semi-immersed Jarlan-Type perforated breakwaters, *China Ocean Eng.*, 29(6), 793–806.

Losada, I.J., Losada, M.A. and Baquerizo, A., 1993. An analytical method to evaluate the efficiency of porous screens as wave dampers, *Appl. Ocean Res.*, 15(4), 207–215.

Molin, B., Lécuye, B. and Remy, F., 2009. Hydrodynamic modelling of partial dikes, *Proceedings of the 24th International Workshop on Water Waves and Floating Bodies*, Zelenogorsk, Russia.

Natale, L., 1983. Reduction of clapotis in front of perforated breakwaters, *Giornale del Genio Civile*, 246–256. (in Italian)

Neelamani, S. and Vedagiri, M., 2002. Wave interaction with partially immersed twin vertical barriers, *Ocean Eng.*, 29(2), 215–238.

Sawaragi, T. and Iwata, K., 1978. Wave attenuation of a vertical breakwater with two air chambers, *Coast. Eng. Japan*, 21, 63–74.

Suh, K.D. and Park, W.S., 1995. Wave reflection from perforated-wall caisson breakwaters, *Coast. Eng.*, 26(3), 177–193.

Suh, K.D., Choi, J.C., Kim, B.H., Park, W.S. and Lee, K.S., 2001. Reflection of irregular waves from perforated-wall caisson breakwaters, *Coast. Eng.*, 44(2), 141–151.

Suh, K.D., Park, J.K., and Park, W.S., 2006. Wave reflection from partially perforated-wall caisson breakwater, *Coast. Eng.*, 33(2), 264–280.

Tanimoto, K. and Yoshimoto, Y., 1982. Theoretical and experimental study of reflection coefficient for wave dissipating caisson with a permeable front wall, *Report of the Port and Harbour Research Institute*, 21(3), 44–77. (in Japanese)

Twu, S.W. and Lin, D.T., 1991. On a highly effective wave absorber, *Coast. Eng.*, 15(4), 389–405.

Yu, X.P., 1995. Diffraction of water waves by porous breakwaters, *J. Waterw. Port Coast Ocean Eng.*, 121(6), 275–282.

Williams, A.N., Mansour, A.E.M. and Lee, H.S., 2000. Simplified analytical solutions for wave interaction with absorbing-type caisson breakwaters, *Ocean Eng.*, 27(11), 1231–1248.